Experimental and theoretical studies of Λ doublings and permanent electric dipoles in the low-lying $^1\Pi$ states of NaCs

J. Zaharova, O. Nikolayeva, M. Tamanis, M. Auzinsh, and R. Ferber[a)]
Department of Physics, University of Latvia, Riga LV-1586, Latvia and Institute of Atomic Physics and Spectroscopy, University of Latvia, Riga LV-1586, Latvia

A. Zaitsevskii, E. A. Pazyuk, and A. V. Stolyarov
Department of Chemistry, Moscow State University, Moscow 119899, Russia

(Received 24 February 2006; accepted 22 March 2006; published online 11 May 2006)

We present experimental data on the electric permanent dipole moments $d(v',J')$ and Λ splittings (q factors) in the quasidegenerate (3) $^1\Pi_{e/f}$ state of the NaCs molecule over a wide range of the vibrational (v') and rotational (J') quantum numbers by using the combination of dc Stark mixing and electric radio frequency-optical double resonance methods. Within the experimental (3) $^1\Pi$ state v' ranged from $v'=0$ to 34, q values exhibited a pronounced decrease from 7.91×10^{-6} to 0.47×10^{-6} cm^{-1}, while $|d|$ values varied between 8.0 and 5.0 D. Experimental evaluation yielded small d values about 1 D for $D(2)$ $^1\Pi$ state $v'<3$ levels. The experiment is supported by *ab initio* electronic structure calculations performed for the (1–3) $^1\Pi$ states of NaCs by means of the many-body multipartitioning perturbation theory of potential energy curves, permanent dipole, and angular coupling matrix elements for the lowest singlet states. The predicted d values reproduce their experimental counterparts within the measurement errors while theoretical q factors reproduce the measured v' dependence being, however, systematically overestimated by ca. 1×10^{-6} cm^{-1}. The present NaCs data are compared with those of the NaK and NaRb molecules. © *2006 American Institute of Physics*. [DOI: 10.1063/1.2196407]

I. INTRODUCTION

Excited states of polar heteronuclear alkali diatomic molecules are currently an object of intensive studies mainly devoted to the search to produce ultracold polar molecules from various species. This, in turn, is particularly appealing due to possible application in quantum computation, fundamental tests of the electron dipole moment, etc. Formation of the first ultralcold molecules has been recently demonstrated for RbCs (Refs. 1 and 2) and KRb.[3] For further development there is an acute need for detailed spectroscopic information on the excited state behavior in a wide range of internuclear distances R. From a management viewpoint, there is an undoubted interest in dynamic parameters such as permanent dipole moments, electronic transition probabilities, and lifetimes.

In the case of the NaCs molecule, the highly accurate experimental potential energy curve[4,5] (PEC) and permanent electric dipole moment[6] (PEDM) are available for the ground state. The experimental spectroscopic information on the excited state PECs are rather limited while their dynamic parameters have not been determined at all. The $D(2)$ $^1\Pi$ state which dissociates to the Na($3s$)+Cs($5d$) limit of separated atoms, see Fig. 1, was studied in Ref. 4 by Doppler-free polarization spectroscopy yielding a set of Dunham coefficients and Λ doubling constants, which are, however applicable only for the lower unperturbed vibronic levels. The third excited (3) $^1\Pi$ state has been recently investigated[7] by Fourier transform spectroscopy (FTS), yielding an accurate PEC covering 95% of the potential well. A theoretical study on the NaCs molecule was performed in Ref. 8 for the 32 lowest electronic states over a wide R range by means of nonempirical pseudopotentials and full valence configuration interaction (CI) calculations of the adiabatic PECs.

The present work continues a series of investigations, both experimental and theoretical, on polar alkali diatomic molecules which started with NaK,[9,10] then NaRb,[11] and RbCs,[12] and continuing here with the NaCs molecule. As for NaK and NaRb, a very high PEDM value reaching $d=7.5$ D was discovered for the covalent D $^1\Pi$ states which converge to the Na($3p$)+K($4s$) and Na($3p$)+Rb($5s$) dissociation limits, respectively. The next logical step is to study the $^1\Pi$ state in the NaCs molecule dissociating to the Na($3p$)+Cs($6s$) atomic limit, namely, the third (3) $^1\Pi$ state, see Fig. 1. For this state one may predict a large PEDM value d_{NaCs} up to 8 D by a linear extrapolation of the experimental d_{NaK} and d_{NaRb} values with respect to the dipole polarizabilities of the ground states of the K, Rb, and Cs atoms. It looked feasible to apply to the (3) $^1\Pi$ NaCs state the method used in Refs. 9 and 10 based on combining dc Stark effect and electric radio frequency (rf)–optical double resonance (ODR). This became possible due to the appearance of high accuracy empirical spectroscopic data on the (3) $^1\Pi$ state of the NaCs molecule.[7]

The paper is organized as follows. In Sec. II we present a background of the method, experimental details, and results. The *ab initio* calculations on the potential energy curves, dipole moment functions, and angular coupling ma-

[a)]Electronic mail: ferber@latnet.lv

 © 2006 American Institute of Physics

Downloaded 15 May 2006 to 130.183.84.47. Redistribution subject to AIP license or copyright, see http://jcp.aip.org/jcp/copyright.jsp

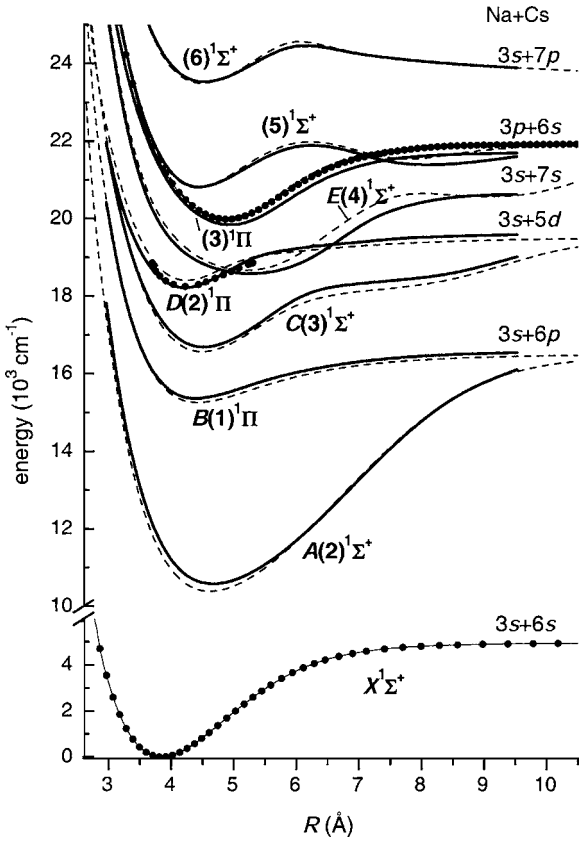

FIG. 1. Schema of adiabatic potential energy curves for the low-lying $^1\Sigma$ and $^1\Pi$ states of the NaCs molecule. Full circles denote the empirical PECs available for the ground $X\,^1\Sigma^+$ (Ref. 5), $D(2)\,^1\Pi$ (Ref. 4), and $(3)\,^1\Pi$ (Ref. 7) states. The excited states solid and dashed lines correspond to "difference-based" PECs constructed from the present MPPT and pseudopotential curves of Ref. 8, respectively.

trix elements for the $(1-3)\,^1\Pi$ and $(1-6)\,^1\Sigma^+$ states, as well as their transformation to the PEDMs and q factors as dependent on vibrational quantum number v' are presented in Sec. III. Finally, in Sec. IV we discuss the obtained experimental and theoretical results and compare them with those for other polar alkali dimers.

II. EXPERIMENT

A. Outline of method

The diatomic molecules in a quasidegenerate $\Lambda \neq 0$ state with a fixed rotational level $J' \geqslant \Lambda$ usually possess a small Λ splitting $\Delta_{e/f}$ into two different e/f parity components[13] which are not interacting with each other in an isolated molecule.[14] In the presence of an external electric field E the e and f sublevels are mixed via the Stark interaction operator $\hat{\mathbf{H}}_{\mathrm{St}}=\mathbf{dE}$. It leads to the appearance of "forbidden" lines in the $^1\Pi \rightarrow {}^1\Sigma^+$ laser induced fluorescence (LIF) spectrum which contains the complete P,Q,R-triplet fluorescence series instead of either P,R doublets or Q singlets (see Fig. 2 for an example). In other words, the intensity of the forbidden I_f lines is borrowed from the "parent" I_p lines in the presence of a dc electric field. The expected $I_f(E)/I_p(E)$ ratio was calculated using density matrix formalism for the interaction of cw broadband radiation with a diatomic molecule in the presence of an external electric field.[9,15] The required

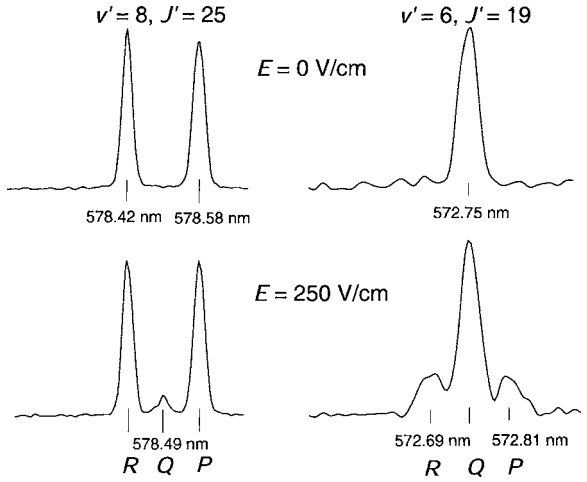

FIG. 2. Examples of the appearance of "forbidden" lines in the $(3)\,^1\Pi \rightarrow X\,^1\Sigma^+$ LIF spectrum after applying a dc electric field. (a) for the "parent" P,R lines; (b) for the "parent" Q line.

Stark energies were obtained by accounting for the $J \pm \Delta J$ mixing ($\Delta J \leqslant 3$) within a given v' state. As was proven, the E dependence of the $I_f(E)/I_p(E)$ ratio is governed by a single parameter $|\Delta_{e/f}/d|$ within a sufficiently wide parameter range. Hence, the E dependence of the I_f/I_p ratio observed for a definite linear polarization of exciting laser beam and LIF at certain excitation/observation directions, see Fig. 3, allows one to obtain the $|\Delta_{e/f}/d|$ ratio of the upper $(v',J')\,^1\Pi$ state, see Refs. 9–11 for more details.

The Λ splitting $\Delta_{e/f}$ value is apparently needed in order to derive the d value from the ratio $|\Delta_{e/f}/d|$. The required Λ splitting is most often determined by conventional spectroscopic analysis of high resolution rovibronic spectra corresponding, as a rule, to rather high rotational levels. The analysis of high resolution FTS spectra for the $(3)\,^1\Pi$ state of NaCs performed in Ref. 7 yielded q factor values and sign; however, their accuracy was rather moderate, especially for J' values below 30. In the present study more accurate $|\Delta_{e/f}|$ values are obtained directly by the rf-ODR method applied earlier in Refs. 10 and 11. The essence of the method is as follows. A certain position of a forbidden line of the LIF progression originating from the upper v',J' level is singled out by the monochromator in the presence of a dc external electric field. Then, instead of a dc field, a radio frequency electric field scanned in frequency ν_{rf}, typically over a 10^6-10^9 Hz range, is applied to the Stark plates causing the appearance of the forbidden line which reaches its maximal intensity when ν_{rf} hits the resonance condition $\nu_{\mathrm{rf}}=|\Delta_{e/f}|$. The resonance signal, see Fig. 4, may be approximated by a Lorentzian contour.[16] The measured Λ splitting and $|\Delta_{e/f}/d|$ ratio yield the absolute value of $d(v',J')$ for a particular rovibronic v',J' level of a $^1\Pi$ state. The $\Delta_{e/f}$ value also yields, in the second order perturbation theory,[14] the corresponding q factor value $|q|=|\Delta_{e/f}|/J'(J'+1)$ which is expected to be a smooth function of v' and J'. Such a combination of dc Stark and electric rf-ODR measurements allows one to determine only the absolute magnitude of the PEDMs and q factors while their signs are not determined.

Downloaded 15 May 2006 to 130.183.84.47. Redistribution subject to AIP license or copyright, see http://jcp.aip.org/jcp/copyright.jsp

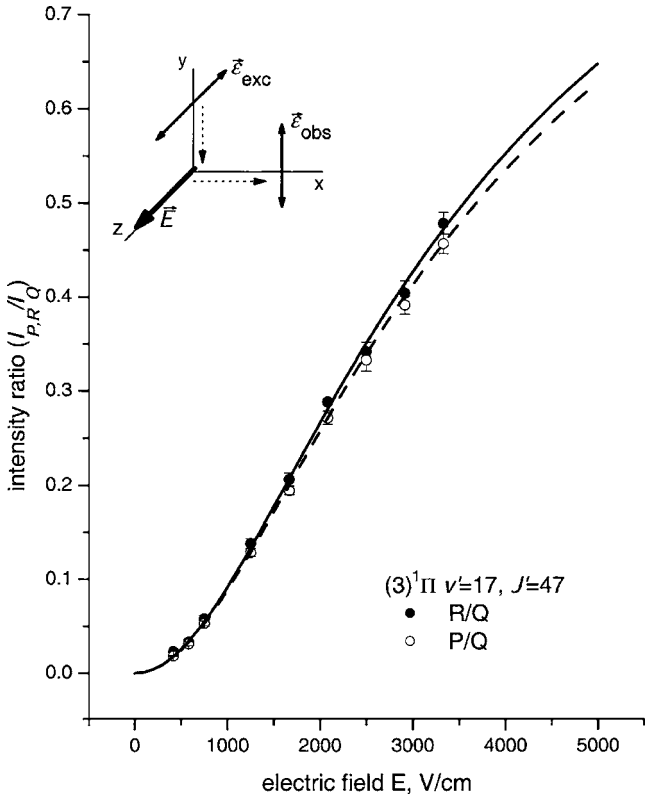

FIG. 3. Experimental electric field dependence of "forbidden" to "parent" LIF lines intensity ratio I_R/I_Q (full circles) and I_P/I_Q (open circles). The respective solid and dashed lines correspond to the best fit yielding $|\Delta_{e/f}/d|=5.48\times10^{-7}$ cm^{-1}/D. **E**, $\boldsymbol{\varepsilon}_{exc}$, and $\boldsymbol{\varepsilon}_{obs}$ denote external electric field, exciting light, and LIF polarization directions, respectively.

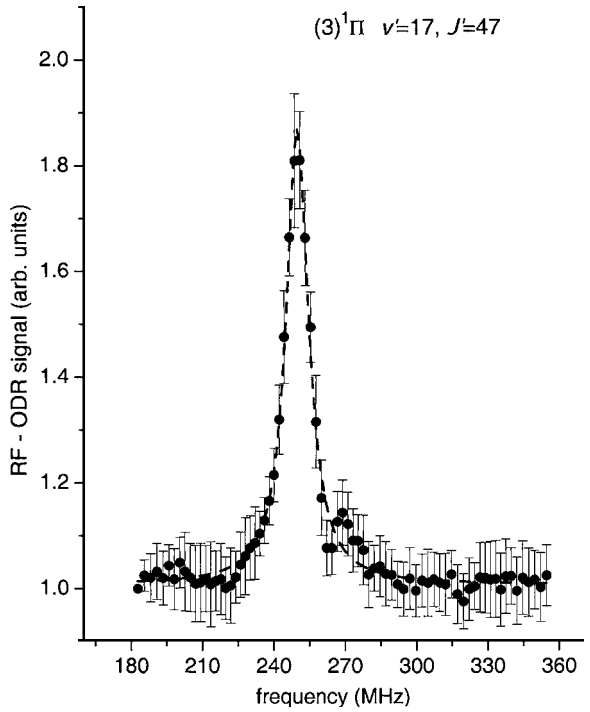

FIG. 4. Experimental rf-ODR signal for (3) $^1\Pi$ state $v'=17$, $J'=47$ level approximated by a Lorentzian contour (dashed line).

B. Experimental details

NaCs molecules were formed from ca. 1:1 mixture (by weight) of Na and Cs metals in a thermal alkali-resistant glass cell at temperatures of 550–570 K. Overall eight different excitation wavelengths λ^{exc} within the range of 465.8–528.7 nm produced by an Ar^+ laser (Spectra Physics 171 and Spectra Physics BeamLok 2040E) operating in the multimode regime were used to excite (3) $^1\Pi\leftarrow X\,^1\Sigma^+$ transitions in NaCs. A tunable single mode dye laser (Coherent CR 699-21) with rhodamine 6G dye was used to excite the $D(2)\,^1\Pi$ state v',J' levels, see Table I. The subsequent LIF radiation emitted at right angles to the laser propagation direction has been dispersed by a double monochromator DFS-12 with 1200 lines/mm gratings and 5 Å/mm inverse dispersion in first diffraction order, providing a 0.2 Å spectral resolution at reasonable slit widths. Fluorescence was detected in the spectral range of 480–600 nm by a FEU-79 photomultiplier tube operating in the photon counting regime. An electric field up to $E=4500$ V/cm was applied to carefully polished stainless steel Stark electrode disks 0.6 cm in diameter separated by a 1.2 ± 0.1 mm gap.

Direct rf-ODR measurements of the $|\Delta_{e/f}|$ values have been performed in the following way. The rf oscillating electric field was generated by a set of MiniCircuits POS voltage controlled oscillators providing a frequency range $\nu_{rf}=22-1000$ MHz. A controlled POS driving voltage was obtained from a digital-analog convertor (DAC) of CAMAC system, which, in its turn, has been driven by a personal computer (PC). The rf signal from POS after passing a MiniCircuits amplifier (Model ZHL-2-12) was applied to the Stark plates. The rf electric field amplitude at the Stark plates was typically 2-3 V, slightly varying with frequency. Frequency calibration by a frequency meter was done prior to the experiment by measuring the frequencies corresponding to DAC numbers used in the experiment.

C. Results

The observed (3) $^1\Pi\rightarrow X\,^1\Sigma^+$ LIF progressions from the particular (3) $^1\Pi$ state v',J' rovibronic level, see Table I, were assigned with a help of FTS data obtained recently in Ref. 7 since exactly the same LIF series excited by the laser lines λ^{exc} have been used. The $D(2)\,^1\Pi\leftarrow X\,^1\Sigma^+$ excitation frequencies needed to excite the desired v',J' levels were calculated using empirical PECs for the ground $X\,^1\Sigma^+$ state[5] and Dunham coefficients for the $D(2)\,^1\Pi$ state.[4]

After choosing the appropriate spectral region which is free of alien fluorescence lines of other origin, the dc electric field was applied. Polarizers were used to provide a definite linear polarization of LIF and laser excitation, see the insert in Fig. 3. The e/f Stark mixing in the excited $(v',J')\,^1\Pi$ state was detected by measuring the relative intensity I_f/I_p of extra (forbidden) Q or P,R lines as demonstrated in Fig. 2. The intensity ratio I_f/I_p was determined by a Gaussian approximation of the spectral line profile after accounting for the spectral background. In some cases residual forbidden line intensity has been observed at zero electric field, most probably due to the collisional e/f mixing. In such a case the residual intensity has been subtracted from the respective $I_f(E)$ values. An example of the recorded $I_f(E)/I_p(E)$ ratio dependence on electric field is presented in Fig. 3. As can be seen, the experimental accuracy allows one to distinguish the

Downloaded 15 May 2006 to 130.183.84.47. Redistribution subject to AIP license or copyright, see http://jcp.aip.org/jcp/copyright.jsp

TABLE I. Ar^+ laser excitation lines λ^{exc} (in nm) or dye laser frequencies υ^{exc} (in cm^{-1}), experimental term values $T_{\upsilon' J'}$ (in cm^{-1}), absolute value $|q|$ of q factors (in 10^{-6} cm^{-1}), and permanent electric dipole moments $|d|$ (in Debye) for the particular rovibronic υ', J' levels of the NaCs $^1\Pi$ state excited from the $(\upsilon'', J'')X\,^1\Sigma^+$ state.

3 $^1\Pi$ state							
λ^{exc}	υ'	J'	υ''	J''	$T_{\upsilon' J'}$	$\lvert q\rvert$	$\lvert d\rvert$
528.6	0	22	11	22	20 30.3088	7.91±0.11	7.5±0.6
514.5	3	45	7	45	20 268.7331	7.35±0.03	7.4±0.4
501.7	6	19	4	19	20 385.9281	7.72±0.18	7.5±0.4
501.7	7	53	4	54	20 532.7184	6.60±0.02	8.0±0.4
496.5	8	25	3	24	20 511.3682	6.48±0.10	7.6±0.5
488.0	13	39	2	39	20 821.1696	4.97±0.04	7.2±0.4
488.0	17	47	4	47	21 053.0013	3.69±0.03	6.8±0.4
488.0	18	66	4	66	21 175.1748	3.66±0.02	6.7±0.5
476.5	21	75	0	75	21 357.7807	2.90±0.01	—
472.7	22	25	0	26	21 239.7082	2.23±0.10	6.7±0.3
472.7	23	50	0	50	21 346.0771	2.01±0.03	6.1±0.4
476.5	25	67	2	68	21 493.8446	1.82±0.02	5.8±0.4
465.8	34	46	1	47	21 740.0677	0.47±0.05	5.0±0.5
$D(2)\,^1\Pi$ state							
υ^{exc}, cm^{-1}	υ'	J'	υ''	J''	$T_{\upsilon' J'}$	$\lvert q\rvert$[a]	$\lvert d\rvert$
17 557.77	0	24	7	23	18 311.77	11.5	1.2±0.4
17 713.40	1	20	6	21	18 368.24	6.68	0.7±0.2

[a]Reference 4.

small difference in $I_f(E)/I_p(E)$ intensity ratios of R- and P-type "forbidden" lines. The experimental dependences were fitted with the calculated ones by varying the $|\Delta_{e/f}/d|$ parameter. A reasonable value of the excited level relaxation rate $\Gamma = 5\times 10^7$ s^{-1}, see discussion in Sec. IV, was used in calculations. It was numerically proved that changes in the $|\Delta_{e/f}/d|$ parameter obtained from fitting did not exceed 1% when Γ was changed by an order of magnitude.

An example of the rf-ODR signal is presented in Fig. 4. The Lorentzian approximation of the measured signals yielded directly the experimental $|\Delta_{e/f}|$ values which were transformed to q factors (see Table I and Fig. 5). A positive sign for the rf-ODR q factors was assumed basing on the FTS data from Ref. 7, which means $T(J_e) > T(J_f)$ using $\Delta_{e/f} = T(J_e) - T(J_f)$ as the definition of Λ splitting. The q value error limits given in Table I account for inaccuracies in the calibration of the frequency meter as well as for minor random variations between different measurements.

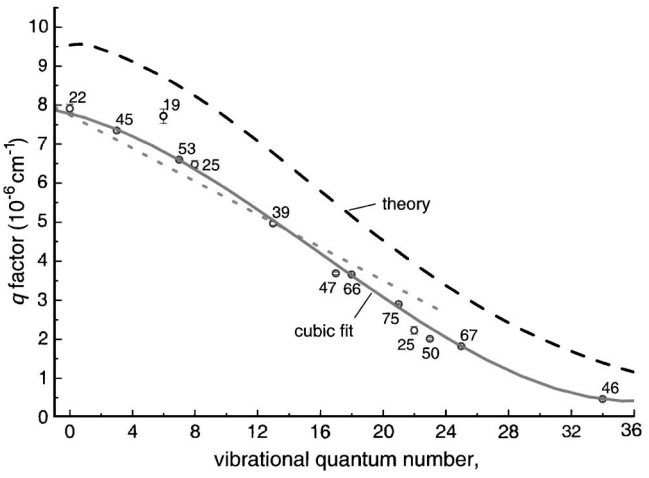

FIG. 5. The (υ', J') (3) $^1\Pi$ state q values measured by rf-ODR (open circles, numbers denote J' values) fitted by a third order polynomial (5) (solid line). The dotted line presents a linear fit of FTS q values from Ref. 7 while the dashed line depicts present MPPT calculations.

The experimental (3) $^1\Pi$ state $|d|$ values obtained by combining the $|\Delta_{e/f}|$ values and $|\Delta_{e/f}/d|$ ratios are presented in Table I and depicted in Fig. 6. The d error estimates in the table account for the $\Delta_{e/f}$ error, inaccuracy in measuring the electric voltage, as well as for random variations of d values obtained in different experiments. Additional systematic error persists from the uncertainty in the gap between the Stark plates.

The forbidden to "allowed" intensity ratio E dependences have been measured also for three υ', J' levels of the $D(2)\,^1\Pi$ state of NaCs, namely, for $\upsilon'=0$, $J'=24$, $\upsilon'=1$, $J'=20$, and $\upsilon'=3$, $J'=21$, using dye laser excitation. Unfortunately, all attempts to get any reliable rf-ODR signal for these levels failed, probably because of small d values for the $D(2)\,^1\Pi$ state (see Fig. 7). Therefore to estimate PEDMs in the $D(2)\,^1\Pi$ state we used the required q values from Ref. 4, see Table I. The resulting $D\,^1\Pi$ state d values for $\upsilon'=0$ and 1 are given in Table I.

III. CALCULATION

A. Outline of method

Ab initio adiabatic PECs $U^{ab}(R)$ of low-lying singlet states of NaCs, dipole moment functions $d^{ab}(R) = \langle \Psi^{el}_{\Pi} | \mathbf{d}_z | \Psi^{el}_{\Pi} \rangle$ for the three lowest (1–3) $^1\Pi$ states, as well as angular momentum coupling matrix elements $L^{ab}_{\Pi-\Sigma}(R) = \langle \Psi^{el}_{\Pi\pm} | [\mathbf{L}_x \pm \mathbf{L}_y]/\sqrt{2} | \Psi^{el}_{\Sigma} \rangle$ between the (1–3) $^1\Pi$ and the six lowest $^1\Sigma^+$ states were calculated by means of the many-

Downloaded 15 May 2006 to 130.183.84.47. Redistribution subject to AIP license or copyright, see http://jcp.aip.org/jcp/copyright.jsp

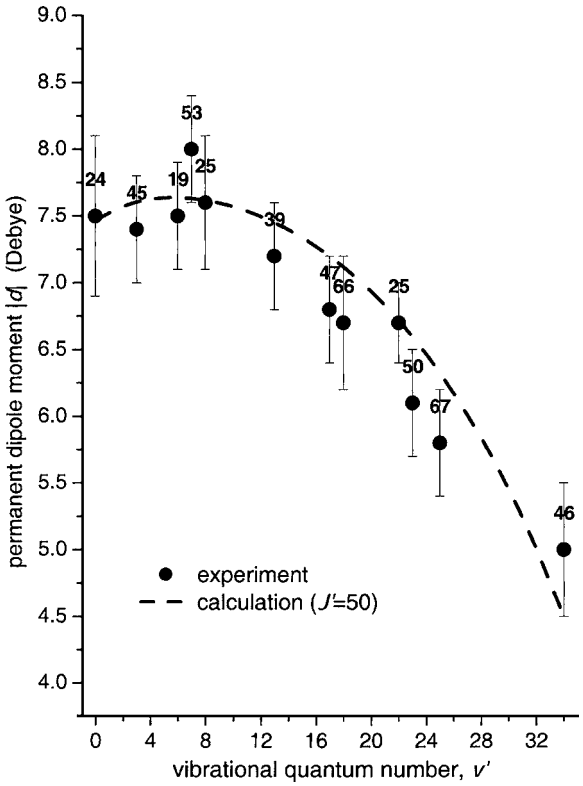

FIG. 6. Experimental (circles, numbers denote J' value) and theoretical (for $J'=50$, dashed line) permanent electric dipole moments $|d|$ for the (3) $^1\Pi$ state.

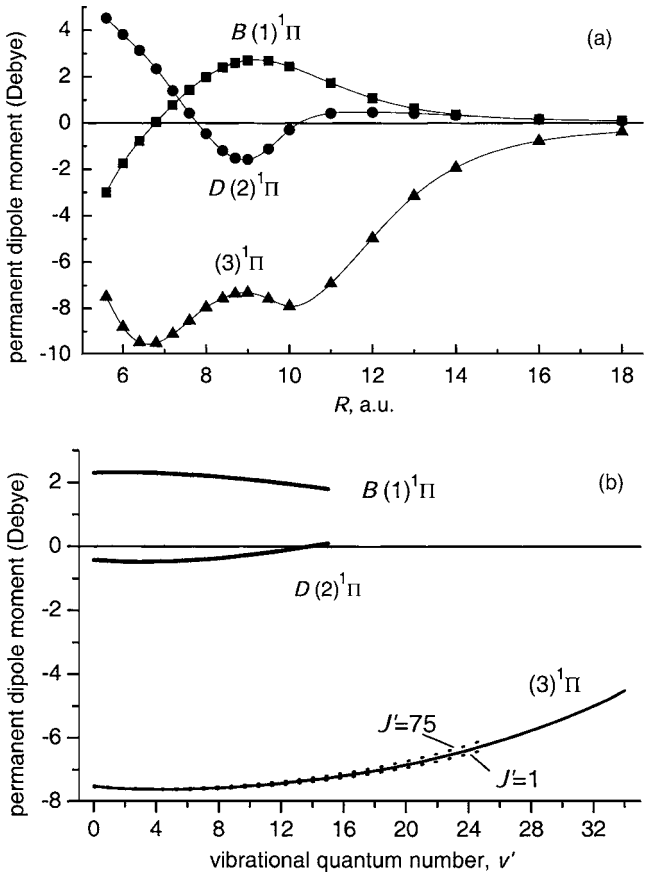

FIG. 7. Calculated permanent electric dipole moments for the $(1-3)\ ^1\Pi$ states. (a) $d(R)$ function; (b) $d(v')$ function. The dotted lines represent calculations for $J'=1$ and $J'=75$ while the solid line represents calculations for $J'=50$. Negative d values indicate Na^+Cs^- polarity.

body multipartitioning perturbation theory[17,18] (MPPT) at internuclear distances $R \in 5.6$ and 18.0 a.u. The computational scheme was very similar to that employed recently for the RbCs molecule.[12] The present calculations were performed in the framework of the pure Hund's case *a* coupling scheme,[14] while spin independent relativistic effects were taken into account by replacing the inner atomic core [Kr]4*d* (Ref. 10) of Cs by the spin-averaged shape-consistent relativistic pseudopotential.[19] Atomic Gaussian basis sets $[(15s10p5d3f)/[8s6p5d3f]$ with contracted inner functions for Na and uncontracted $(8s7p6d3f)$ for Cs] were obtained by appropriate extension of the basis from Refs. 19 and 20, respectively (see also Ref. 21 for details). Outer-core molecular orbitals were obtained via state-averaged Monte Carlo self-consistent field (MCSCF) calculations on the lowest $^{1,3}\Sigma$ states of the neutral molecule and $^2\Sigma^+$ states of the positive ion; during the generation of the remainder molecular orbitals (MOs) the averaging was restricted to the ionic states. Electronic energies and valence wave functions were obtained from the state-selective effective Hamiltonian constructed in the full valence (two-electron) configuration interaction space; the core-valence correlation and residual core polarization effects were incorporated through perturbative evaluation of effective valence-shell interactions in second order. Permanent dipole values and angular momentum matrix elements were derived from one-particle spin-free transition density matrices computed at the first MPPT order.[22] The evaluation and transformation of the requisite molecular integrals and complete active space self-consistent field (CASSCF) calculations were performed by means of the COLUMBUS quantum chemistry software[23,24] while the MPPT calculations were carried out by the diagrammatic PT code DiagPT.[18]

The adiabatic potentials U_i^{ab} computed for the excited states were transformed to their "difference-based" counterparts U_i^{dif} through the simple relation,[25]

$$U_i^{dif}(R) = U_X^{IPA}(R) + [U_t^{ab}(R) - U_X^{ab}(R)], \quad (1)$$

where $U^{IPA}(R)$ is the highly accurate empirical potential for the ground state.[5] Due to cancellation of the systematic R dependent errors (in particular, basis set superposition errors) the "difference-based" PECs constructed for the excited NaCs states by the present MPPT and pseudopotential curves of Ref. 8 (see Fig. 1) usually agree with the empirical potentials better than the original *ab initio* curves.

The *ab initio* permanent electric dipole moment functions $d^{ab}(R)$ for the $(1-3)\ ^1\Pi$ states are presented in Fig. 7(a) while the angular momentum coupling matrix elements between the (3) $^1\Pi$ and $(1-6)\ ^1\Sigma^+$ states are depicted in Fig. 8. The complete tables of the original MPPT PECs for the $(1-3)\ ^1\Pi$ and $(1-6)\ ^1\Sigma^+$ states, the corresponding difference-based potentials of the excited states, dipole moments of the $(1-3)\ ^1\Pi$ states, and *L*-coupling matrix elements between $(1-3)\ ^1\Pi$ and $(1-6)\ ^1\Sigma^+$ states are available from the EPAPS archive.[21]

Downloaded 15 May 2006 to 130.183.84.47. Redistribution subject to AIP license or copyright, see http://jcp.aip.org/jcp/copyright.jsp

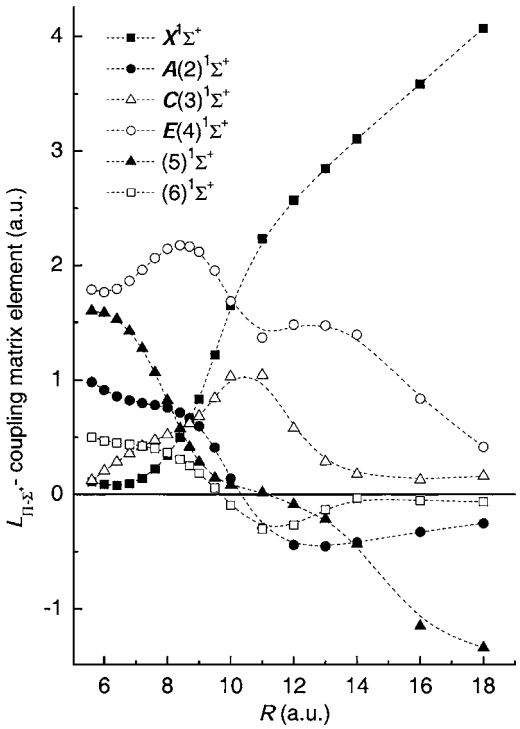

FIG. 8. *Ab initio* *L*-coupling matrix elements between the (3) $^1\Pi$ and (1–6) $^1\Sigma^+$ states.

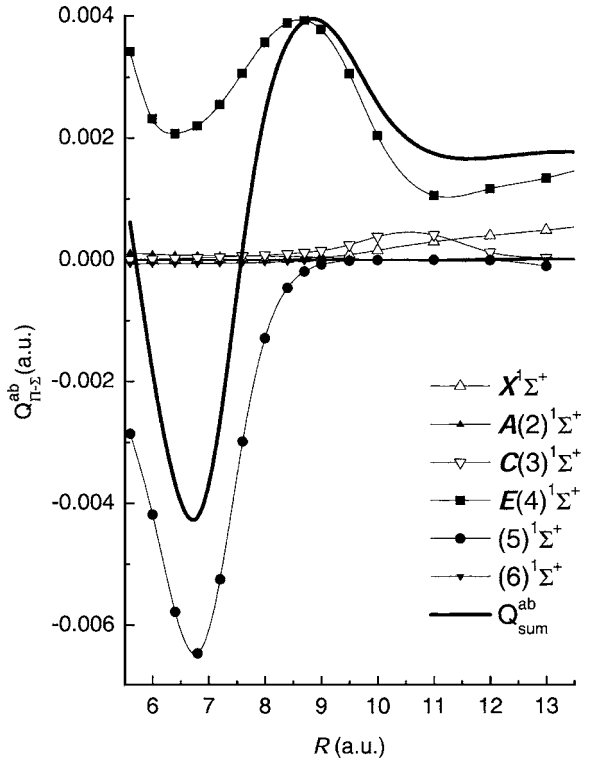

FIG. 9. Partial contributions $Q^{ab}_{\Pi-\Sigma}(R)$ of the six lowest $^1\Sigma^+$ states into the q factor of the (3) $^1\Pi$ state.

B. Permanent electric dipole moments $d(v',J')$ and q factors $q(v',J')$

Permanent electric dipole moments for the particular rovibronic levels of the (1–3) $^1\Pi$ state were evaluated as the expectation value of the *ab initio* function $d^{ab}(R)$,

$$d(v,J) = \langle v^J_\Pi | d^{ab}(R) | v^J_\Pi \rangle. \tag{2}$$

The rovibrational wave functions $|v^J_\Pi\rangle$ in Eq. (2) were obtained by a numerical solution of the radial Schrödinger equation with the empirical PEC for the (3) $^1\Pi$ state of NaCs from Ref. 7 and *ab initio* $U^{dif}_i(R)$ potentials for the (1–2) $^1\Pi$ states. Calculated $d(v)$ dependences for all three lowest $^1\Pi$ states are presented in Fig. 7(b). A comparison of $|d(v')|$ for the (3) $^1\Pi$ state with the present experiment is shown in Fig. 6.

The q factors of the $^1\Pi$ state have to be evaluated, by definition, as the double infinite sums over all bound and embedding continuum rovibronic $^1\Sigma^+$ states,[14]

$$q(v,J) = \frac{1}{\mu^2} \sum_{\Sigma^+} \sum_{v_\Sigma} \frac{|\langle v^J_\Pi | L^{ab}_{\Pi-\Sigma}(R)/R^2 | v^J_\Sigma \rangle|^2}{E^{vJ}_\Pi - E^{v_\Sigma J}_\Sigma}, \tag{3}$$

where μ is the reduced molecular mass while E^{vJ}_i and $|v^J_i\rangle$ are the rovibrational eigenvalues and eigenfunctions of the interacting adiabatic states. In practice, the present q factor calculation for the (3) $^1\Pi$ state was restricted to the sum over the lowest six $^1\Sigma^+$ states while tedious explicit consideration of the complete vibrational eigenstate problem for the $^1\Sigma^+$ states has been avoided by the approximate sum rules,[26,27]

$$q(v,J) \approx \frac{1}{\mu^2} \left\langle v^J_\Pi \left| R^{-4} \sum_{\Sigma^+} Q^{ab}_{\Pi-\Sigma}(R) \right| v^J_\Pi \right\rangle,$$
$$Q^{ab}_{\Pi-\Sigma} = |L^{ab}_{\Pi-\Sigma}(R)|^2 / \Delta U^{ab}_{\Pi-\Sigma}(R), \tag{4}$$

where the $\Delta U^{ab}_{\Pi\Sigma} = U^{ab}_\Pi - U^{ab}_{\Sigma^+}$ is the difference between the corresponding *ab initio* PECs. A singularity of Eq. (4) caused by the crossing of the (3) $^1\Pi$ and (5) $^1\Sigma^+$ PECs at the point $R_x \approx 7.0$ Å, see Fig. 1, was eliminated by a smoothing cubic spline fitting[28] of the relevant $Q^{ab}_{(3)\,^1\Pi-(5)\,^1\Sigma^+}(R)$ function. The resulting q-factors are presented in Fig. 5 while the corresponding $Q^{ab}_{(3)\,^1\Pi-(5)\,^1\Sigma^+}(R)$ functions are depicted in Fig. 9.

IV. DISCUSSION AND CONCLUSIONS

The calculated (3) $^1\Pi$ state PEDM values $d(v')$ demonstrate weak dependence on rotational quantum number J' within the J' range involved, see Fig. 7(b). The theoretically predicted $d(v')$ behavior in the v',J' range under study is therefore represented, within ca. 1%, by the calculated dependence for $J'=50$, see dashed line in Fig. 6. One can notice that the measured PEDMs agree with their theoretical counterparts within the error bars. As it might be expected, the absolute value and negative sign (assuming Na^+Cs^- polarity) of the calculated PEDMs [see Fig. 7(b)] for the NaCs molecule in the (3) $^1\Pi$ state converging to the Na(3*p*) +Cs(6*s*) limit is very close to those for the *D* $^1\Pi$ state of NaK (Ref. 10) and NaRb (Ref. 11) dimers converging to Na(3*p*)+K(4*s*) and Na(3*p*)+Rb(5*s*) limits, respectively. The

Downloaded 15 May 2006 to 130.183.84.47. Redistribution subject to AIP license or copyright, see http://jcp.aip.org/jcp/copyright.jsp

calculated PEDMs for the NaCs $B(1)\ ^1\Pi$ are close to the respective values of NaK (Ref. 10) and NaRb (Ref. 11) as well.

The calculated NaCs $(3)\ ^1\Pi$ state q factors demonstrate a steep decrease with v', see Fig. 5. At the same time, calculations did not reveal any pronounced J' dependence of the q factors. The largest difference between q factors was at $v'=0$ yielding, for instance, a q value for $J'=50$ only 2% smaller than for $J'=1$; the difference becomes negligible for $v'>10$. This allows one to compare the theoretically estimated $q(v')$ function with the experimentally observed $q(v')$ dependence obtained at different J' values, see Fig. 5.

The absence of J dependence within the J' range involved, which was confirmed also by the experimental q values obtained in Ref. 7 from FTS data, allows one to include the $q(v')$ dependence in a weighted (by experimental errors) polynomial fit. It appears feasible to use a third order polynomial,

$$q(v') = q_0 + q_1 v' + q_2 (v')^2 + q_3 (v')^3, \tag{5}$$

yielding $q_0=(7.79\pm0.05)\times10^{-6}\ \mathrm{cm}^{-1}$, $q_1=(-10.36\pm1.07)\times10^{-8}\ \mathrm{cm}^{-1}$, $q_2=(-1.13\pm0.06)\times10^{-8}\ \mathrm{cm}^{-1}$, and $q_3=(2.35\pm0.11)\times10^{-10}\ \mathrm{cm}^{-1}$.

For comparison, the linear fit of the experimental NaCs $(3)\ ^1\Pi$ state q values obtained from the FTS data in Ref. 7 as $q(v')=q_0+q_1v'$ with $q_0=(7.74\pm0.13)\times10^{-6}\ \mathrm{cm}^{-1}$ and $q_1=(-2.115\pm0.088)\times10^{-7}\ \mathrm{cm}^{-1}$ is plotted in Fig. 5, demonstrating satisfactory agreement with the present measurements. One may note that the FTS usually yields a broad scope of q values within a wide range of v' and J' (except for small J' values) while the rf-ODR measurements provide better accuracy, however, being more time consuming and providing a limited q factor data field. Besides, rf-ODR signals allow one to estimate the lifetimes, see, for instance, Ref. 29. We did not intend to elaborate on the rf-ODR signal shape for the lifetime measurements; however, a crude estimate, accounting for collisions with Cs atoms, yields a lifetime value about 40 ns. It should be reminded that the obtained q_i parameters are valid within the observed v' region and are not recommended for extrapolation.

The calculated v' dependence of q factors, see dashed line in Fig. 5, reproduces the shape of the present empirical dependence (5). However, the calculated values are systematically overestimated by an almost constant value. The observed systematic deviation seems to be attributed to the uncertainty of the *ab initio* PECs for the nearest $(4)\ ^1\Sigma^+$ and $(5)\ ^1\Sigma^+$ states which provide the main contribution to the q factor of the $(3)\ ^1\Pi$ state due to the minimal energy gap at small internuclear distances (see Fig. 1). Other possible reasons for the discrepancy come from a residual contribution of the higher-lying $(n>6)\ ^1\Sigma^+$ states and from the approximate summation estimated by the relation (4).

The NaCs $(3)\ ^1\Pi$ state q factor values being of the order of $10^{-5}\ \mathrm{cm}^{-1}$ for small v' are comparable to the ones in the $D\ ^1\Pi$ state of NaK (Ref. 22) and NaRb.[25,30] While the latter are weakly dependent on v' within the v' range under study, the NaCs $(3)\ ^1\Pi$ state q factors demonstrate a very steep decrease with v', see Fig. 5. This can be explained by the fact that the NaCs $(3)\ ^1\Pi$ state q factors are determined, according to Fig. 9, by a strong competition between the partial contributions of the nearest higher lying state $(5)\ ^1\Sigma^+$ and nearest lower-lying state $(4)E\ ^1\Sigma^+$, see Fig. 1. In other words, the "*unique perturber*" approximation,[14] which is partly valid for the $D\ ^1\Pi$ state of NaK and NaRb, completely fails for the $(3)\ ^1\Pi$ state of NaCs. Moreover, the L-coupling matrix elements $\sqrt{2}<L_{\Pi-\Sigma}<\sqrt{6}$ calculated at small internuclear distances between the $(3)\ ^1\Pi$ and $(4,5)\ ^1\Sigma^+$ states of NaCs (see Fig. 8) clearly indicate that the well-known Van-Vleck hypothesis of a *"pure precession"*[14] breaks down, which is due to the pronounced l mixing of the p and d orbitals. This l-mixing effect caused by the strong dipolar core[31] rapidly increases for NaK, NaRb, and NaCs dimers due to the increasing shift of the center of mass origin with respect to a nonzero angular momentum atom. The abrupt variations of the *ab initio* $L^{ab}_{\Pi\sim\Sigma^+}(R)$ functions observed at the intermediate internuclear distances can be attributed to strong configuration interaction between the higher-excited $^1\Sigma^+$ states converging to the different $NaCs^+$ core states.

The q factor calculation for the lowest vibrational level $v'=0$ of the NaCs $D(2)\ ^1\Pi$ state yields $q=+1.08\times10^{-5}\ \mathrm{cm}^{-1}$. This result is remarkably close to its experimental counterpart $+1.15\times10^{-5}\ \mathrm{cm}^{-1}$ obtained from the conventional Dunham fit of the Doppler-free $D(2)\ ^1\Pi\leftarrow X\ ^1\Sigma^+$ polarization spectra.[4] The present analysis, see also Ref. 21, confirms quantitatively the assumption in Ref. 4 that the main contribution to the q factor of the $D\ ^1\Pi$ state comes from the lower-lying $(3)\ ^1\Sigma^+$ state converging to the same $Na(3s)+Cs(5d)$ dissociation limit, see Fig. 1. As far as the NaCs $D(2)\ ^1\Pi$ state PEDMs are concerned, the experimental d values estimated for $v'=0$ and 1, see Table I, agree within the error bars with the theoretically predicted ones, see Fig. 7(b). At the same time an experimental estimate for the $v'=3$ level, yielding 4 ± 2 D, disagrees with the calculated value of ca. 0.4 D. This discrepancy can be explained by the fact that the q value required for the estimates of $\Delta_{e/f}$ and d was obtained by extrapolation of Ref. 4 data. Such extrapolation is obviously not valid since the $D(2)\ ^1\Pi$ state is strongly perturbed even at low $v'>2$ as observed in Ref. 4.

ACKNOWLEDGMENTS

The authors are indebted to O. Docenko and Dr. I. Klincare for valuable discussions. The work has been supported by the NATO SfP-978029 Optical Field Mapping grant. Riga team acknowledges support from Latvian State Research Programme "Advanced Inorganic Materials for Photonic and Energetics" (Grant No. 1-23/50). Two of the authors (O.N. and J.Z.) are grateful to European Social Fund for support.

[1] J. M. Sage, S. Sainis, T. Bergeman, and D. DeMille, Phys. Rev. Lett. **94**, 203001 (2005).
[2] A. J. Kerman, J. M. Sage, S. Sainis, T. Bergeman, and D. DeMille, Phys. Rev. Lett. **92**, 153001 (2004).
[3] D. Wang, J. Qi, M. F. Stone, O. Nikolayeva, H. Wang, B. Hattaway, S. D. Gensemer, P. L. Gould, E. E. Eyler, and W. C. Stwalley, Phys. Rev. Lett. **93**, 243005 (2004).
[4] U. Diemer, H. Weickenmeier, M. Wahl, and W. Demtröder, Chem. Phys. Lett. **104**, 489 (1984).
[5] O. Docenko, M. Tamanis, R. Ferber, A. Pashov, H. Knöckel, and E. Tiemann, Eur. Phys. J. D **31**, 205 (2004).
[6] P. J. Dagdigian and L. Wharton, J. Chem. Phys. **57**, 1487 (1973).

Downloaded 15 May 2006 to 130.183.84.47. Redistribution subject to AIP license or copyright, see http://jcp.aip.org/jcp/copyright.jsp

[7] O. Docenko, M. Tamanis, J. Zaharova, R. Ferber, A. Pashov, H. Knöckel, and E. Tiemann, J. Chem. Phys. **124**, 2006 (in press).
[8] M. Korek, A. R. Allouche, K. Fakhreddine, and A. Chaalan, Can. J. Phys. **78**, 977 (2000).
[9] M. Tamanis, M. Auzinsh, I. Klincare, O. Nikolayeva, A. V. Stolyarov, and R. Ferber, J. Chem. Phys. **106**, 2195 (1997).
[10] M. Tamanis, M. Auzinsh, I. Klincare, O. Nikolayeva, R. Ferber, E. A. Pazyuk, A. V. Stolyarov, and A. Zaitsevskii, Phys. Rev. A **58**, 1932 (1998).
[11] O. Nikolayeva, I. Klincare, M. Auzinsh, M. Tamanis, R. Ferber, E. A. Pazyuk, A. V. Stolyarov, A. Zaitsevskii, and R. Cimiraglia, J. Chem. Phys. **113**, 4896 (2000).
[12] A. Zaitsevskii, E. A. Pazyuk, A. V. Stolyarov, O. Docenko, I. Klincare, O. Nikolayeva, M. Auzinsh, M. Tamanis, and R. Ferber, Phys. Rev. A **71**, 012510 (2005).
[13] M. H. Alexander, P. Andresen, R. Bersohn *et al.*, J. Chem. Phys. **89**, 1749 (1988).
[14] H. Lefebvre-Brion and R. W. Field, *The Spectra and Dynamics of Diatomic Molecules* (Academic, New York, 2004).
[15] M. Auzinsh and R. Ferber, *Optical Polarisation of Molecules* (Cambridge University Press, Cambridge, 1996).
[16] R. W. Field and T. H. Bergemann, J. Chem. Phys. **54**, 2936 (1971).
[17] A. Zaitsevskii and J. P. Malrieu, Theor. Chem. Acc. **96**, 269 (1997).
[18] A. Zaitsevskii and R. Cimiraglia, Int. J. Quantum Chem. **73**, 395 (1999).
[19] R. B. Ross, J. M. Powers, T. Atashroo, and W. C. Ermler, J. Chem. Phys. **93**, 6654 (1990).
[20] A. J. Sadlej and M. Urban, J. Mol. Struct.: THEOCHEM **234**, 147 (1991).
[21] See EPAPS Document No. E-JCPSA6-124-008617 for the *ab initio* MPPT potential energy curves (PECs) for the lowest singlet $(1-6)\ ^1\Sigma^+$ and $(1-3)\ ^1\Pi$ states of NaCs molecule, the "difference-based" PECs for the excited singlet states of NaCs constructed with respect to the ground state, *ab initio* MPPT permanent dipole moments for the singlet $(1-3)\ ^1\Pi$ states of NaCs, and the *ab initio* MPPT angular momentum coupling matrix elements between the $(1-3)\ ^1\Pi$ and $(1-6)\ ^1\Sigma^+$ states of NaCs. This document can be reached via a direct link in the online article's HTML reference section or via the EPAPS homepage (http://www.aip.org/pubservs/epaps.html).
[22] S. O. Adamson, A. Zaitsevskii, E. A. Pazyuk, A. V. Stolyarov, M. Tamanis, R. Ferber, and R. Cimiraglia, J. Chem. Phys. **113**, 8589 (2000).
[23] R. Shepard, I. Shavitt, R. M. Pitzer, D. C. Comeau, M. Pepper, H. Lischka, P. G. Szalay, R. Ahlrichs, F. B. Brown, and J. G. Zhao, Int. J. Quantum Chem. **22**, 149 (1988).
[24] H. Lischka, R. Shepard, I. Shavitt *et al.*, COLUMBUS, an *ab initio* electronic structure program, release 5.8, 2001.
[25] A. Zaitsevskii, S. O. Adamson, E. A. Pazyuk, A. V. Stolyarov, O. Nikolayeva, O. Docenko, I. Klincare, M. Auzinsh, M. Tamanis, R. Ferber, and R. Cimiraglia, Phys. Rev. A **63**, 052504 (2001).
[26] A. V. Stolyarov and V. I. Pupyshev, Phys. Rev. A **49**, 1693 (1994).
[27] E. A. Pazyuk, A. V. Stolyarov, and V. I. Pupyshev, Chem. Phys. Lett. **228**, 219 (1994).
[28] C. H. Reinsch, Numer. Math. **10**, 177 (1967).
[29] M. Tamanis, M. Auzinsh, I. Klincare, O. Nikolayeva, R. Ferber, A. Zaitsevskii, E. A. Pazyuk, and A. V. Stolyarov, J. Chem. Phys. **109**, 6725 (1998).
[30] O. Docenko, M. Tamanis, R. Ferber, A. Pashov, H. Knöckel, and E. Tiemann, Eur. Phys. J. D **36**, 49 (2005).
[31] M. S. Child, in *Molecular Rydberg Dynamics* (Imperial College Press, London, 1999), pp. 1–16.

Downloaded 15 May 2006 to 130.183.84.47. Redistribution subject to AIP license or copyright, see http://jcp.aip.org/jcp/copyright.jsp